

Supplemental Information

**Interactome Mapping Provides a Network of
Neurodegenerative Disease Proteins and Uncovers
Widespread Protein Aggregation in Affected Brains**

Christian Haenig, Nir Atias, Alexander K. Taylor, Arnon Mazza, Martin H. Schaefer, Jenny Russ, Sean-Patrick Riechers, Shushant Jain, Maura Coughlin, Jean-Fred Fontaine, Brian D. Freibaum, Lydia Brusendorf, Martina Zenkner, Pablo Porras, Martin Stroedicke, Sigrid Schnoegl, Kristin Arnsburg, Annett Boeddrich, Lucia Pigazzini, Peter Heutink, J. Paul Taylor, Janine Kirstein, Miguel A. Andrade-Navarro, Roded Sharan, and Erich E. Wanker

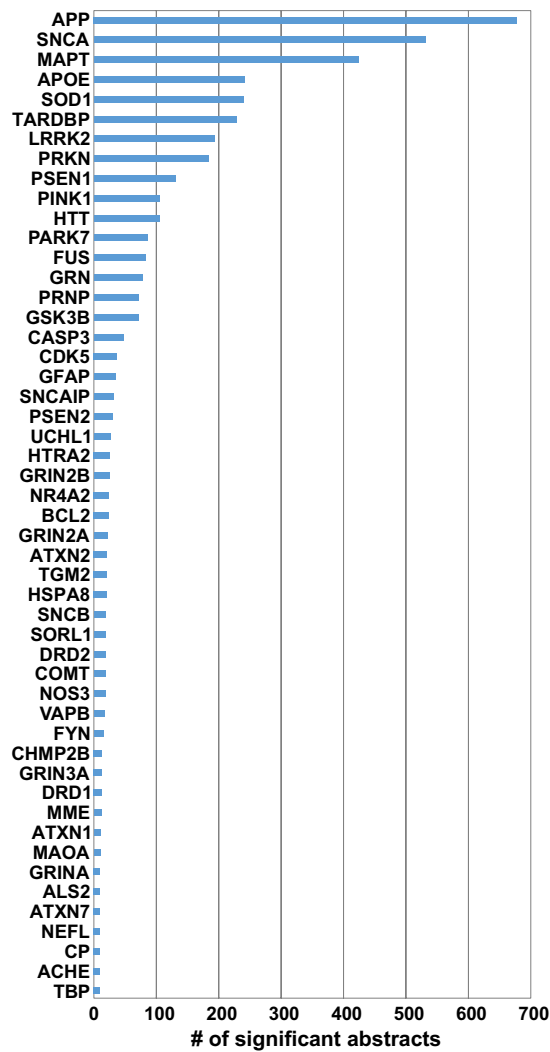


Figure S1. Related to Figure 1. Text mining for initially selected targets

Number of significant abstracts retained from a literature search using the Génie text mining algorithm (Fontaine et al., 2011) for the top 50 of the initially selected targets. We searched for abstracts that contain both a selected target gene as well as the search term "neurodegeneration". Only a relatively small fraction of the selected target genes (~ 20) has been extensively described in the context of neurodegenerative diseases.

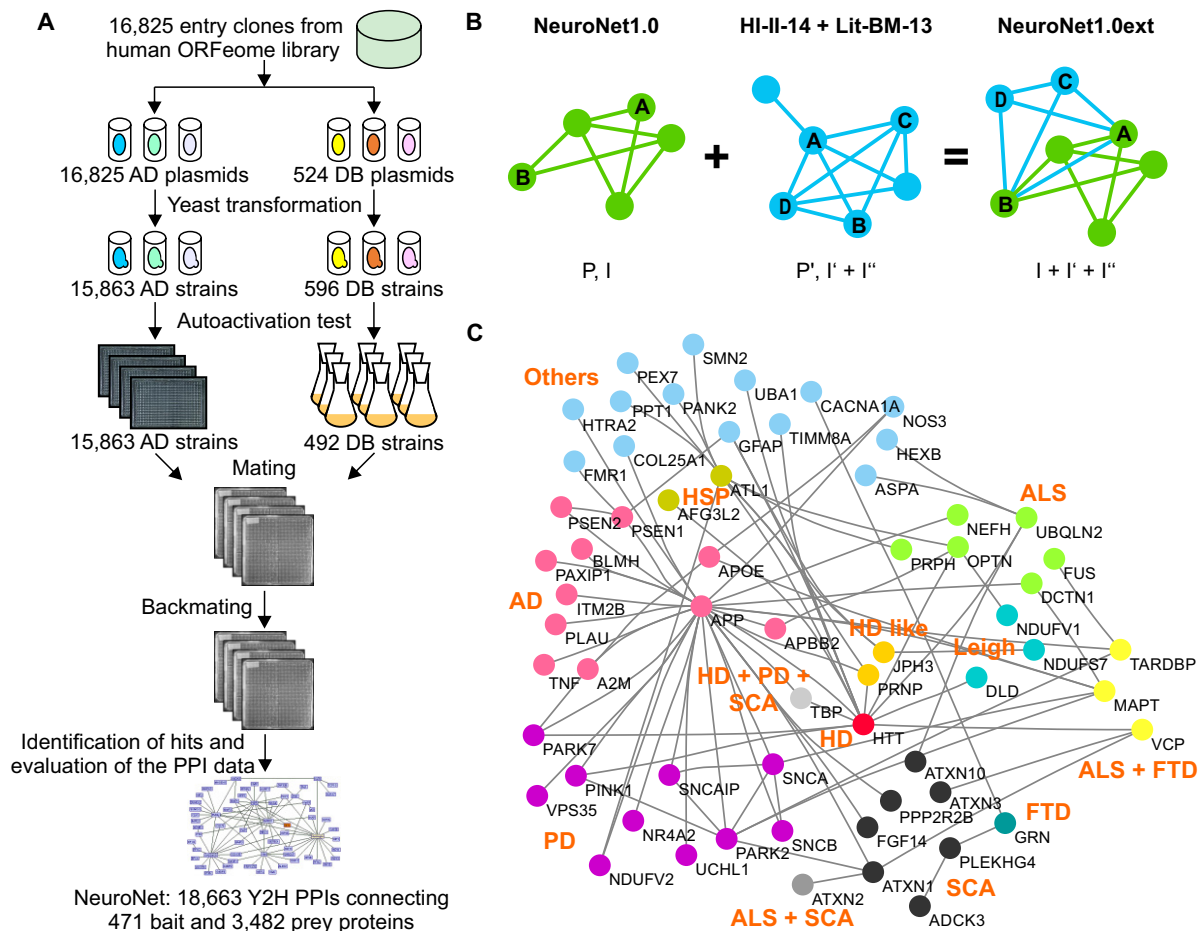


Figure S2. Related to Figure 1. Identification of PPIs and integration of binary Y2H interaction data sets

(A) Simplified workflow depicting the automated Y2H interaction mating technology. DB, DNA binding domain; AD, activation domain.

(B) Scheme depicting the integration of binary Y2H interaction data. The Y2H interactions identified in this study (NN1.0) were extended with previously published high-quality PPIs (Lit-BM-13 and HI-II-14) to generate NN1.0ext. The following PPI integration strategy was applied: Let P be the set of proteins (e.g., A, B) in NN1.0 and let I denote its set of interactions. Let P' be the set of proteins (e.g., C, D) in the Lit-BM-13 and the HI-II-14 collections that have at least two PPIs (e.g., C-A, C-B, D-A, D-B) to proteins in P . Let I' be the set of interactions from the Lit-BM-13 and the HI-II-14 collections that connect proteins in P' to proteins in P or P' . Finally, let I'' be the set of interactions from the Lit-BM-13 and the HI-II-14 collections that connect proteins in P . Then, NN1.0ext is the union of I , I' and I'' .

(C) A subnetwork obtained from the NN1.0ext data set depicting interactions between known NDCPs. The network suggests that NDs are related at the molecular level.

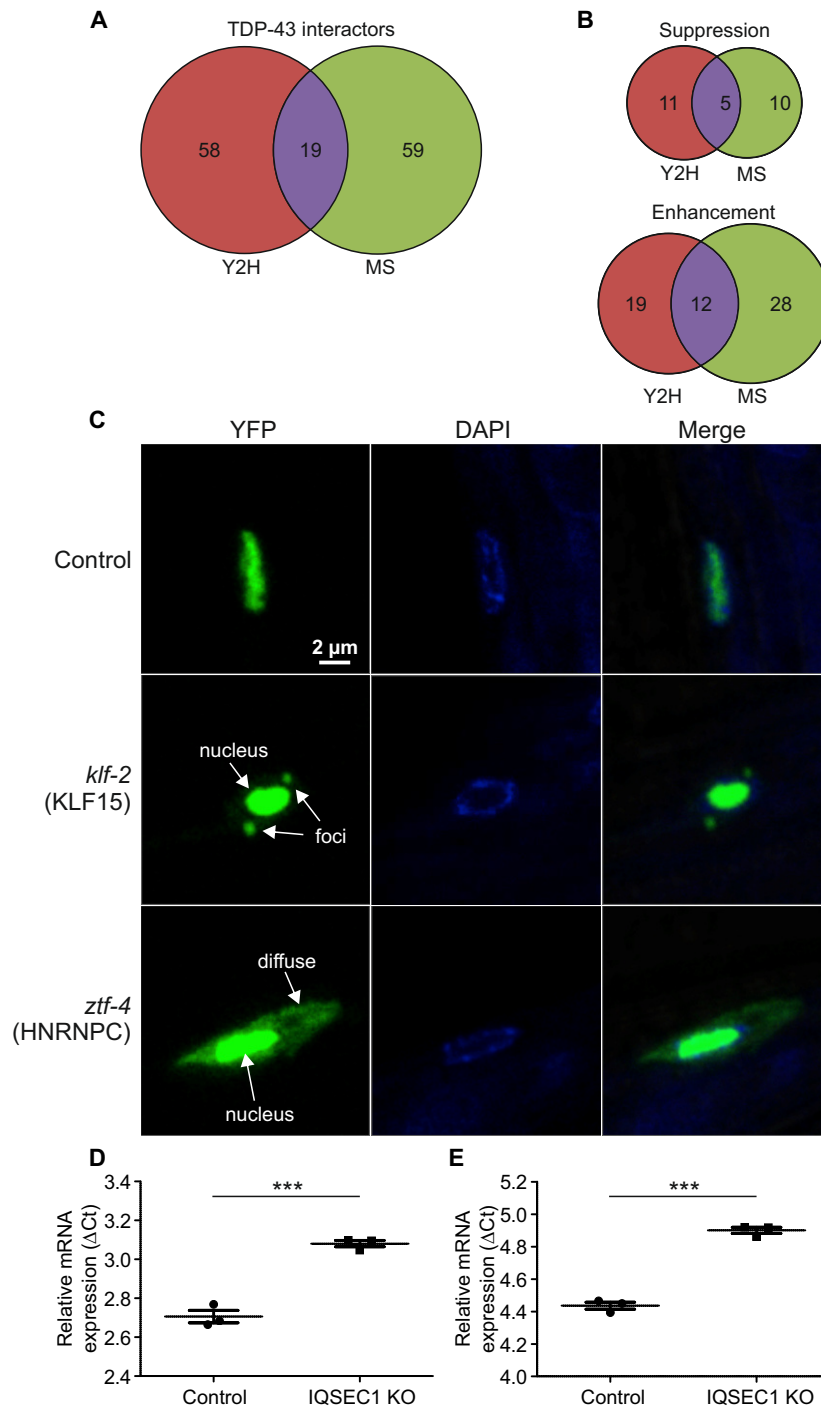


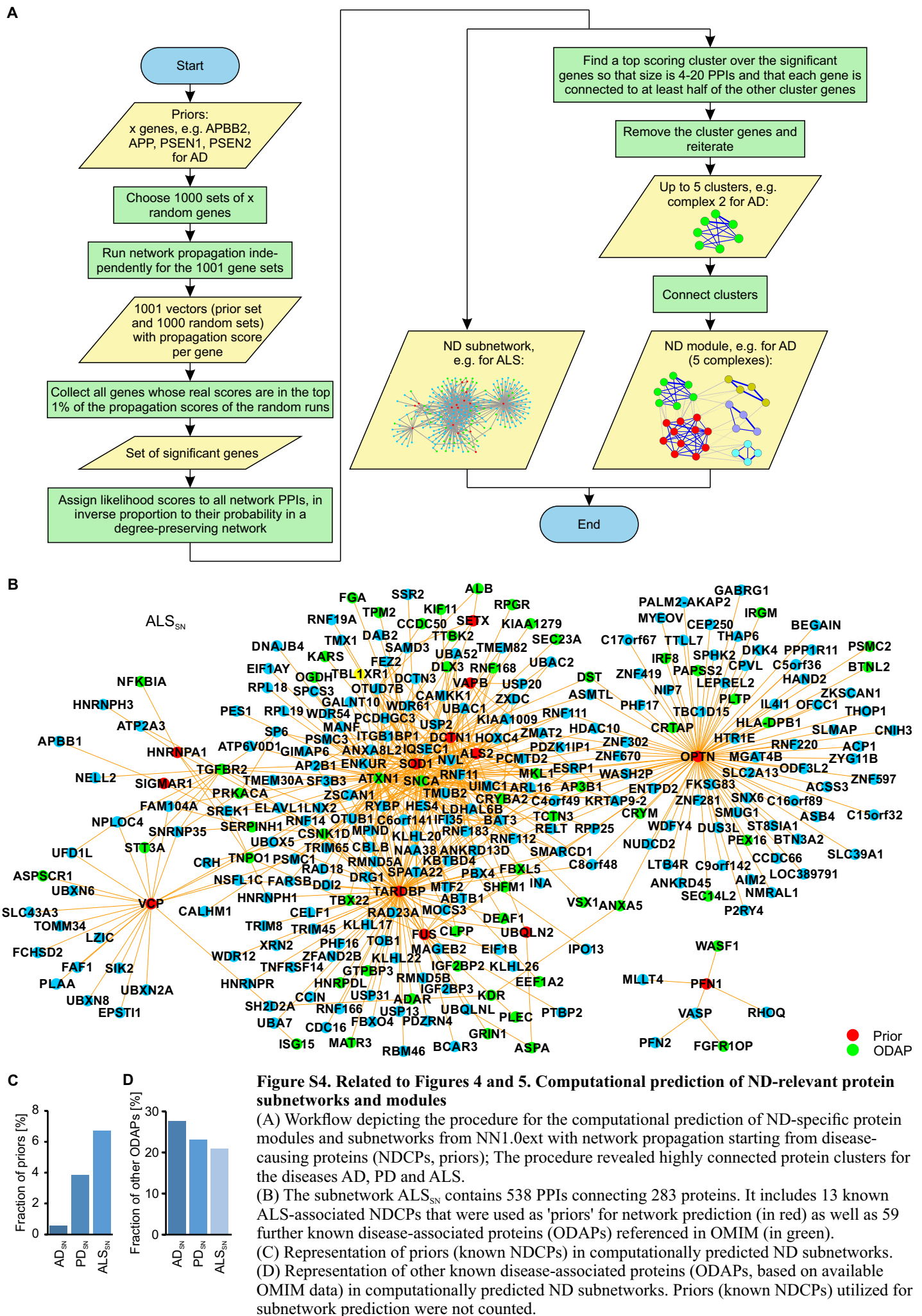
Figure S3. Related to Figures 3 and 6. Investigating the disease relevance of NN1.0ext PPIs in transgenic fly and worm models

(A) Overlap between TDP-43 interacting proteins that were tested with RNAi knockdown experiments in TDP-43-M337V expressing transgenic flies; Y2H, interacting proteins identified with Y2H assays; MS, interacting proteins identified by affinity purification followed by mass spectrometry.

(B) Results from RNAi screens. The impact of partner proteins identified by Y2H assays and affinity purification followed by mass spectrometry (MS) on a TDP-43-M337V-induced rough-eye phenotype in *Drosophila* was systematically assessed.

(C) Cellular TDP-43-M337V-YFP localization phenotype resulting from RNAi knockdown of target genes in a transgenic *C. elegans* model. Observed phenotypes are exemplarily shown. Through the RNAi knockdown of target genes, the translocation of TDP-43-M337V-YFP from the nucleus into the cytoplasm was increased compared to controls, which show exclusively nuclear staining.

(D-E) Quantification of M02B7.5 (IQSEC1) transcript amounts using real-time PCR. RNA was prepared from control and RNAi-treated worms. For PCR two different primer pairs for detecting M02B7.5 transcripts were used. Values were normalised to the *cdc42* housekeeping gene. Statistical analysis was performed using the unpaired two-tailed t-test (** $p < 0.001$).



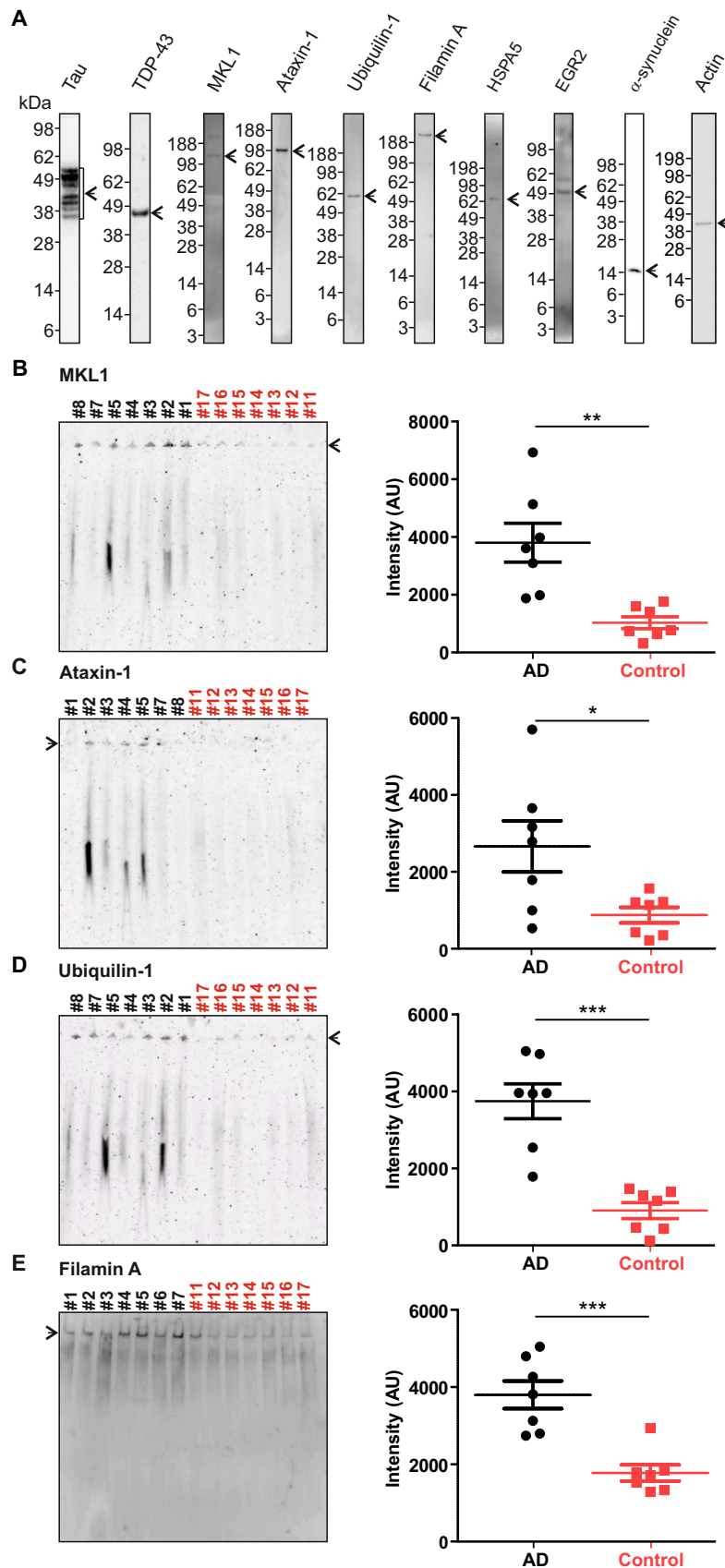


Figure S5. Related to Figure 5. Detection of aggregated proteins in AD patient brains
 (A) Western blot analysis. 10 μ g of human brain homogenates derived from control individuals were analysed by a denaturing NuPAGE gel and Western blotting using protein specific antibodies. Arrows indicate the detected proteins with their predicted sizes.
 (B-E) Analysis of brain extracts by native PAGE. 10 μ g of human brain homogenates derived from 7 AD patients (#1-8, black lettering) and 7 control individuals (#11-17, red lettering) were analysed by native PAGE and Western blotting using antibodies against (B) MKL1, (C) ataxin-1, (D) ubiquilin-1 and (E) filamin A. Intensities of high-molecular-weight protein aggregates in gel pockets (arrow) were quantified using the ImageJ software and are shown in arbitrary units (AU) (** $p < 0.001$, ** $p < 0.01$, * $p < 0.05$, unpaired two-tailed t-test).

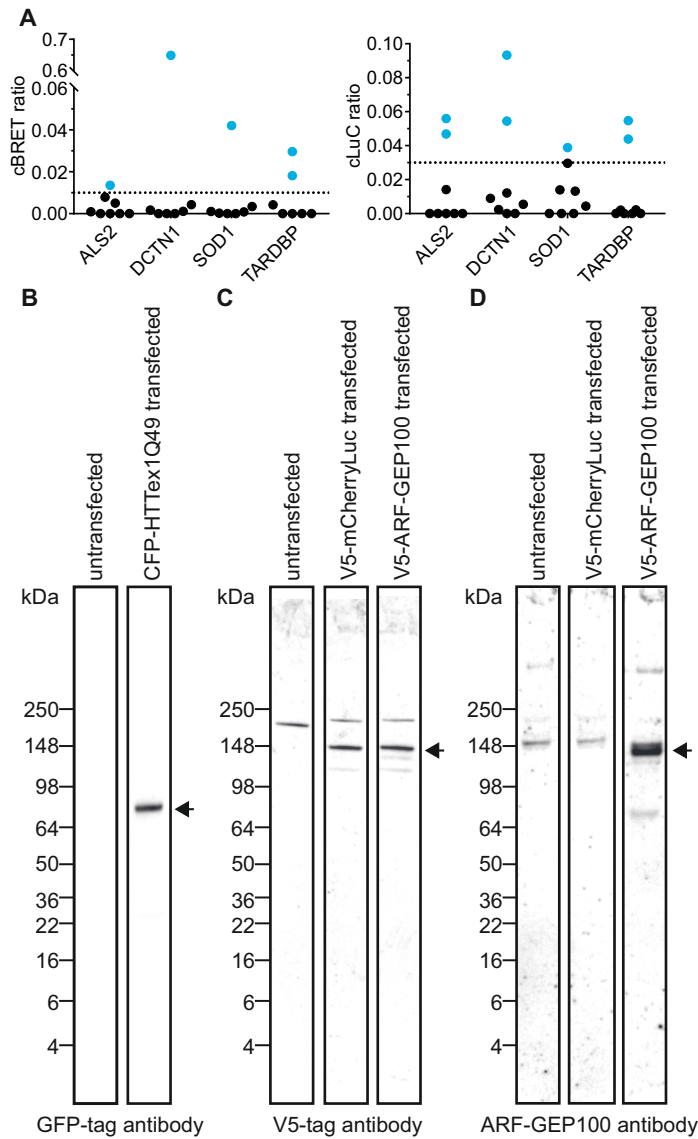


Figure S6. Related to Figures 1, 4 and 6. Systematic analysis of PPIs from the predicted ALS module and of the effect of ARF-GEP100 on CFP-HTTex1Q49 aggregation.

(A) Interacting proteins of ARF-GEP100 from the ALS module were co-expressed as N- and C-terminally tagged NL and PA-mCit fusion proteins in eight different orientations in HEK293 cells. For all orientations cBRET and cLuc ratios were calculated; values (colored in cyan), which are equal or above the thresholds of 0.01 and 0.03, respectively, indicate positive PPIs.

(B-D) Analysis of V5-tagged ARF-GEP100 on CFP-HTTex1Q49 aggregation in HeLa cells by SDS-PAGE and immunoblotting.